

Full Paper

Multiwalled Carbon Nanotubes Encased in Ruthenium Oxide Film as a Hybrid Material for Neurotransmitters Sensor

Chien-Chieh Ti, Yogeswaran Umasankar, Shen-Ming Chen*

Department of Chemical Engineering and Biotechnology, National Taipei University of Technology, No. 1, Section 3, Chung-Hsiao East Road, Taipei 106, Taiwan

*e-mail: smchen78@ms15.hinet.net

Received: January 25, 2009

Accepted: May 13, 2009

Abstract

A hybrid film (MWCNTs-RuO_x·nH₂O) which contains multiwalled carbon nanotubes (MWCNTs) along with the incorporation of ruthenium oxide (RuO_x·nH₂O) has been synthesized on glassy carbon electrode (GCE), gold (Au), indium tin oxide (ITO) and screen printed carbon electrode (SPCE) by potentiostatic methods. The presence of MWCNTs in the hybrid film enhances surface coverage concentration (*T*) of RuO_x·nH₂O to ≈2100%. The surface morphology of the hybrid film deposited on ITO has been studied using scanning electron microscopy and atomic force microscopy. These two techniques reveal that the RuO_x·nH₂O incorporated on MWCNTs. Electrochemical quartz crystal microbalance study too reveals the incorporation of MWCNTs and RuO_x·nH₂O. The MWCNTs-RuO_x·nH₂O hybrid film exhibits promising enhanced electrocatalytic activity towards the biochemical compounds such as epinephrine and norepinephrine. The electrocatalytic responses of these analytes at RuO_x·nH₂O, MWCNTs and MWCNTs-RuO_x·nH₂O hybrid films have been measured using cyclic voltammetry. The obtained sensitivity values from electrocatalysis studies of analytes for MWCNTs-RuO_x·nH₂O hybrid film are higher than the RuO_x·nH₂O and MWCNTs films. Finally, the flow injection analysis has been used for the amperometric studies of analytes at MWCNTs-RuO_x·nH₂O hybrid film modified SPCEs.

Keywords: Multiwall carbon nanotubes, Metal oxides, Modified electrodes, Electrocatalysis, Epinephrine, Norepinephrine, Nanotubes, Thin films

DOI: 10.1002/elan.200904628

1. Introduction

Ruthenium and other metal hybrid materials received great attention in the last few years as high specific surface anodes for electrochemical sensor applications [1–10]. It is a known fact that, the direct electrochemical behavior of bare glassy carbon electrode (GCE) does not show relatively large difference of peak potentials; also the formed sensors show very low sensitivity. To overcome this limitation, several steps had been taken for the fabrication of metal oxides and metal particle hybrid materials, which have been used for enhancing sensing applications. Such kind of materials includes gold [11, 12], SiO₂ nanoparticles, etc [13, 14]. Among these materials, metal oxide electrodes have shown some advantages in electrochemical analysis; and micro- or nano-metal-oxides exhibit unique performance in electric, optical, magnetic and catalytic aspects [15]. Ruthenium based ferrocyanides had also been used as potential electrode material for the electroanalysis [16–18], electrochromism [19], ion-exchange reactions [20], photoelectrochemical, photocatalytic devices, batteries and capacitors [21].

Other than metal oxides, varieties of applications of CNT matrices for the detection of inorganic and bioorganic compounds were already reported [22–24]. Even though,

electrocatalytic activity of the metal oxides and CNT matrices individually shows good result; some properties like mechanical stability, sensitivity for different techniques and electrocatalysis of multiple compounds are found to be poor. To overcome this difficulty, new studies have been developed in the past decade by preparing hybrid films composed of both CNTs and metal oxides. The rolled-up graphene sheets of carbon exhibit a π -conjugative structure with a highly hydrophobic surface. This unique property of CNTs allows them to interact with some compounds through π - π electronic and hydrophobic interactions and form new structures [25, 26]. There were past attempts in the preparation of hybrid and sandwiched films for electrocatalytic studies such as selective detection of dopamine in the presence of ascorbic acid [27]. The sandwiched films were also been used for the designing of nanodevices with the help of non-covalent adsorption, electrodeposition, etc [28]. Similar previous studies on CNT-metal oxide hybrids show the necessity of metal oxide on the CNTs, such as improvement in functional properties like orientation, enhanced electron transport, high capacitance, etc. [29–31].

Epinephrine (EP) and norepinephrine (NEP) are the important catecholamine neurotransmitters in the mammalian central nervous system, which plays very important role in the function of central nervous, renal, hormonal and

cardiovascular system. The catecholamine drugs were used to treat hypertension, bronchial asthma, organic heart disease, and used in cardiac surgery and myocardial infarction [32, 33]. The oxidation of these compounds is interesting as this process occurs in the human body. Due to their crucial role in neurochemistry and industrial applications, several traditional methods have been used for its determination, among them; the electrochemical methods have more advantages over the other in sensing the neurotransmitters in living organisms.

The literature survey reveals that there were no attempts reported for the electroanalysis of EP and NEP at CNT with metal oxide hybrid materials. In this paper, we report about a novel hybrid film (MWCNTs-RuO_x·nH₂O) made of multiwalled carbon nanotubes (MWCNTs) which is incorporated with ruthenium oxide (RuO_x·nH₂O). MWCNTs-RuO_x·nH₂O hybrid film's characterization, enhancement in functional properties, peak current and electrocatalytic activity towards EP and NEP have also been reported. The film formation process involves the modification of GCE with uniformly well dispersed MWCNTs, and which is then modified with RuO_x·nH₂O.

2. Experimental

2.1. Materials and Apparatus

RuCl₃·xH₂O, MWCNTs (*OD* = 10–20 nm, *ID* = 2–10 nm and length = 0.5–200 μm), potassium, EP and NEP obtained from Aldrich and Sigma-Aldrich were used as received. All other chemicals used were of analytical grade. The preparation of aqueous solution was done with twice distilled deionized water. Solutions were deoxygenated by purging with prepurified N₂ gas. The pH 3.0 aqueous solution was prepared from 0.1 M KNO₃. Cyclic voltammetry (CV) was performed in an analytical system model CHI-400 potentiostat. A conventional three-electrode cell assembly consisting of Ag/AgCl reference electrode and a Pt wire counter electrode were used for electrochemical measurements. The working electrode was either an unmodified GCE or a GCE modified with the RuO_x·nH₂O, MWCNTs or MWCNTs-RuO_x·nH₂O hybrid films. In these experiments, all the potentials are reported vs. Ag/AgCl reference electrode. The working electrode for EQCM measurements was an 8 MHz AT-cut quartz crystal coated with gold electrode. The diameter of the quartz crystal is 13.7 mm; the gold electrode diameter is 5 mm. The flow injection analysis (FIA) of the analytes at screen printed carbon electrode (SPCE) were done using Alltech 426 HPLC pump containing an electrochemical cell. The morphological characterization of the films were examined by means of scanning electron microscopy (SEM) (Hitachi S-3000H) and atomic force microscopy (AFM) (Being Nano-Instruments CSPM4000). All the measurements were carried out at 25 °C ± 2.

2.2. Fabrication of MWCNTs-RuO_x·nH₂O Hybrid Film Modified Electrodes

There was an important challenge in the preparation of MWCNTs. Because of its hydrophobic nature, it was difficult to disperse it in any aqueous solution to get a homogeneous mixture. Briefly, the hydrophobic nature of the MWCNTs was converted into hydrophilic nature by following the previous studies [34, 35]. This was done by weighing 10 mg of MWCNTs and 200 mg of potassium hydroxide into a ruby mortar and ground together for 2 h at room temperature. Then, the reaction mixture was dissolved in 10 mL of double distilled deionized water, and then precipitated many times into methanol for the removal of potassium hydroxide. Then, the obtained MWCNTs in 10 mL water were ultrasonicated for 6 h to get a uniform dispersion. This functionalization process of MWCNTs is to get hydrophilic nature, to obtain the homogeneous dispersion of MWCNTs in water. This process not only converts MWCNTs to hydrophilic nature but this helps to breakdown larger bundles of MWCNTs into smaller ones. This was confirmed using SEM, which is not shown in the figures.

Before starting each experiment, GCEs were polished by a BAS polishing kit with 0.05 μm alumina slurry, rinsed and then ultrasonicated in double distilled deionized water. Then, the GCEs were uniformly coated with 50 μg cm⁻² of MWCNTs and dried at room temperature. The electrochemical formation of RuO_x·nH₂O was performed by continuous cycling of potential at the working electrode. The continuous cycling has been performed in a defined potential range of -0.3 to 1.3 V, using 100 mV s⁻¹ scan rate in 0.1 M KNO₃ aqueous solution at pH 3.0, which contains Ru³⁺ ions (1 mM of RuCl₃·xH₂O). Then the MWCNTs-RuO_x·nH₂O hybrid film modified electrode was carefully washed with double distilled deionized water. The concentration of homogeneously dispersed MWCNTs was exactly measured using micro-syringe.

3. Results and Discussion

3.1. Electrochemical Preparation and Characterization of MWCNTs-RuO_x·nH₂O Hybrid Film

Hydrous RuO_x film has been deposited on GCE from 0.01 M RuCl₃·xH₂O present in 0.1 M KNO₃ pH 3.0 electrolyte solution. The typical CVs for the growth of RuO_x·nH₂O film shows two sets of redox peaks in the potential range of -0.3 to 1.3 V (figure not shown). During the negative scan, a peak appears at 0.39 V, which is due to the reduction of Ru³⁺ and thus the deposition of ruthenium (Ru) has taken place on GCE. On the positive sweep, the deposited Ru oxidizes to hydrous oxides (RuO_x·nH₂O) and hydroxyl Ru⁴⁺ species and their corresponding peaks have appeared at about 0.51 V; and the redox couple at *E*^{o'} = 0.15 V represents the Ru^{1+/2+} redox reaction [36, 37]. Following the above growth studies of RuO_x·nH₂O, it has also been deposited on MWCNTs modified GCE at similar pH (0.1 M KNO₃

pH 3.0) using the solution containing Ru^{3+} ions. The scanning potential region for film growth is -0.3 to 1.3 V (Fig. 1a). In this above experiment, upon continuous cycling, the redox peak currents appeared at the formal potentials $E^{\circ'} = 0.15$ and 0.45 V are found to be increasing. This behavior indicates the deposition of $\text{RuO}_x \cdot n\text{H}_2\text{O}$ film during cycling. The electrochemical behavior of $\text{RuO}_x \cdot n\text{H}_2\text{O}$, MWCNTs and MWCNTs- $\text{RuO}_x \cdot n\text{H}_2\text{O}$ hybrid film modified GCEs have been studied after washing them in double distilled deionized water, and transferring them in to pH 3.0 aqueous solution. Figure 1b represents the electrochemical behavior of all the three films, where $\text{RuO}_x \cdot n\text{H}_2\text{O}$ and MWCNTs doesn't possess obvious redox couples. Whereas, MWCNTs- $\text{RuO}_x \cdot n\text{H}_2\text{O}$ hybrid film modified GCE shows overlapped redox couples at $E^{\circ'} = 0.15$ and 0.65 V which reveals the redox reactions of $\text{Ru}^{1+/2+}$ and $\text{Ru}^{3+/4+}$ at MWCNTs- $\text{RuO}_x \cdot n\text{H}_2\text{O}$ hybrid film respectively. Further, comparison of all these films reveals that the MWCNTs- $\text{RuO}_x \cdot n\text{H}_2\text{O}$ hybrid film possesses higher current than $\text{RuO}_x \cdot n\text{H}_2\text{O}$ film. This is due to the more deposition of $\text{RuO}_x \cdot n\text{H}_2\text{O}$ in presence of MWCNTs. These results have been given in Table. 1 in the form of surface coverage concentration values (Γ). The calculated values from the same table shows that, MWCNTs enhances Γ of $\text{RuO}_x \cdot n\text{H}_2\text{O}$ by $84 \text{ pmol cm}^{-2} \mu\text{g}^{-1}$; and the overall increase in percentage of $\text{RuO}_x \cdot n\text{H}_2\text{O}$ Γ at MWCNTs film is 2100%. In this calculation, the charge involved in the reaction (Q) has been obtained from CVs and applied in the equation $\Gamma = Q/nFA$ where, n is the number of electron transfer involved for a redox reaction, and A is the area of working electrode (0.08 cm^2). These above results show that MWCNTs catalyze the $\text{RuO}_x \cdot n\text{H}_2\text{O}$ deposition.

Two similar EQCM experiments have been carried out; one was with bare gold electrode and the other by modifying the gold in electrochemical quartz crystal with uniformly coated MWCNTs and then dried at 40°C . The increase in voltammetric peak current of $\text{RuO}_x \cdot n\text{H}_2\text{O}$ redox couples ($\text{Ru}^{1+/2+}$ and $\text{Ru}^{3+/4+}$) and the frequency decrease (or mass increase) are found to be consistent with the growth of $\text{RuO}_x \cdot n\text{H}_2\text{O}$ film on bare and MWCNTs modified gold electrodes (figures not shown). These results too show that the obvious $\text{RuO}_x \cdot n\text{H}_2\text{O}$ deposition potential starts between -0.3 and 1.3 V. From the frequency change, the change in the mass of $\text{RuO}_x \cdot n\text{H}_2\text{O}$ at bare and MWCNTs modified quartz crystal gold electrode can be calculated by Sauerbrey Equation 1, however 1 Hz frequency change is equivalent to 1.4 ng cm^{-2} of mass change [38, 39]. The mass change during $\text{RuO}_x \cdot n\text{H}_2\text{O}$ incorporation on MWCNTs modified and unmodified gold electrodes for total cycles are 7.04 and $0.5 \mu\text{g cm}^{-2}$, respectively.

$$\text{Mass change } (\Delta m) = -1/2 (f_0^{-2})(\Delta f)A(K\rho)^{1/2} \quad (1)$$

Where, f_0 is the oscillation frequency of the crystal; Δf is the frequency change; A , the area of gold disk; K , the shear modulus of the crystal; ρ , the density of the crystal. Figure 1c indicates the variation of frequency with increase of scan cycles for $\text{RuO}_x \cdot n\text{H}_2\text{O}$ at MWCNTs modified and unmodified

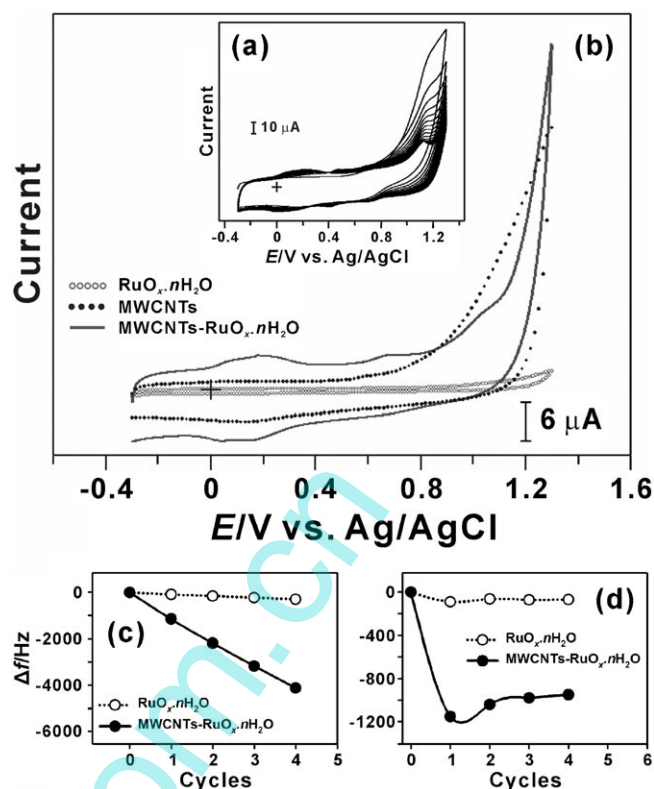


Fig. 1. a) Consecutive CVs of $50 \mu\text{g cm}^{-2}$ MWCNTs-GCE modified from $0.1 \text{ mM RuCl}_3 \cdot x\text{H}_2\text{O}$ present in 0.1 M KNO_3 pH 3 aqueous solution, scan rate at 100 mV s^{-1} . b) CVs of GCE modified from $\text{RuO}_x \cdot n\text{H}_2\text{O}$, MWCNTs and MWCNTs- $\text{RuO}_x \cdot n\text{H}_2\text{O}$ hybrid film, in 0.1 M KNO_3 pH 3 aqueous solution, scan rate at 20 mV s^{-1} . EQCM frequency change responses recorded together with the consecutive CVs ($\text{RuO}_x \cdot n\text{H}_2\text{O}$ formation on MWCNTs modified and unmodified electrode, potential between -0.3 and 1.3 V; scan rate: 20 mV s^{-1}), where c) shows the gross change in the peak current and frequency shift for the first five scan cycles, whereas d) shows the change between each consecutive scans.

modified EQCM gold crystal electrodes. Figure 1d indicates every cycle of frequency with the increase of scan cycles for $\text{RuO}_x \cdot n\text{H}_2\text{O}$ at MWCNTs modified and unmodified EQCM gold crystal electrodes. These EQCM results prove that the deposition of $\text{RuO}_x \cdot n\text{H}_2\text{O}$ on the MWCNTs film is more stabilized and more homogeneous than on the bare gold electrode.

The CVs of $\text{RuO}_x \cdot n\text{H}_2\text{O}$ and MWCNTs- $\text{RuO}_x \cdot n\text{H}_2\text{O}$ hybrid film on GCE in pH 3 at different scan rates reveal that, anodic and cathodic peak currents of the redox couple ($E^{\circ'} = 0.15$ V) for both the films increases linearly with the increase of scan rates (figures not shown). The ratio of I_{pa}/I_{pc} in the same experiments demonstrates that the redox process is not controlled by diffusion for both the films. However, the ΔE_p of each scan rate reveals that the peak separation of hybrid's redox couple ($E^{\circ'} = 0.15$ V) increases as the scan rate increase (figure not shown). From the slope values of ΔE vs. log scan rate, by assuming the value of $\alpha \approx 0.5$, number of electrons involved as one, the electron transfer rate constant (k_s) has been calculated using

Table 1. Surface coverage concentration (Γ) of $\text{RuO}_x \cdot n\text{H}_2\text{O}$ at MWCNTs modified and unmodified GCE using CV technique in pH 3.

Films modified on GCE	Γ (nmol cm^{-2})
$\text{RuO}_x \cdot n\text{H}_2\text{O}$	0.2
MWCNTs- $\text{RuO}_x \cdot n\text{H}_2\text{O}$	4.4

Equation 2 based on Laviron theory [40]. The k_s value is 3.1 cm s^{-1} for MWCNTs- $\text{RuO}_x \cdot n\text{H}_2\text{O}$ hybrid film modified GCE.

$$\log k_s = \alpha \log(1 - \alpha) + (1 - \alpha) \log \alpha - \log(RT/nFv) - \alpha(1 - \alpha)nF\Delta E/2.3RT \quad (2)$$

In the Equation 2, the scan rate and ΔE values are in unit volts. For various pH studies, the MWCNTs- $\text{RuO}_x \cdot n\text{H}_2\text{O}$ hybrid film modified GCE prepared in pH 3 aqueous solution has been washed with deionized water, and has been transferred to various pH aqueous buffer solutions without the presence of $\text{RuCl}_3 \cdot x\text{H}_2\text{O}$ (figures not shown). The results reveal that the film is highly stable in the pH range between 1 and 7, where the values of E_{pa} and E_{pc} depends on the pH value of buffer solution. The formal potential of MWCNTs- $\text{RuO}_x \cdot n\text{H}_2\text{O}$ plotted over the pH range from 1 to 7. The response shows a slope of -59 mV/pH , which is close to that given by Nernstian equation for equal number of electrons and protons transfer. All these above results show the enhanced functional properties of MWCNTs- $\text{RuO}_x \cdot n\text{H}_2\text{O}$ hybrid film in the presence of both $\text{RuO}_x \cdot n\text{H}_2\text{O}$ and MWCNTs.

3.2. Topographic Characterization of MWCNTs- $\text{RuO}_x \cdot n\text{H}_2\text{O}$ Hybrid Film Using SEM and AFM

Three different films; MWCNTs, $\text{RuO}_x \cdot n\text{H}_2\text{O}$ and MWCNTs- $\text{RuO}_x \cdot n\text{H}_2\text{O}$ hybrid films have been prepared on indium tin oxide (ITO) with similar conditions and similar potential as that of GCE and have been characterized using SEM. From Figure 2, it is significant that there are morphological differences between MWCNTs, $\text{RuO}_x \cdot n\text{H}_2\text{O}$ and $\text{RuO}_x \cdot n\text{H}_2\text{O}$ covered MWCNTs films. The top views of structures Figure 2a on the ITO electrode surface shows uniformly coated high concentration of MWCNTs, which completely covered the ITO surface. Similarly, Figure 2b is the deposition of $\text{RuO}_x \cdot n\text{H}_2\text{O}$ on the ITO electrode surface, where the $\text{RuO}_x \cdot n\text{H}_2\text{O}$ forms networks of beads embed together. This above mentioned $\text{RuO}_x \cdot n\text{H}_2\text{O}$ morphology present throughout the entire electrode surface. However, they are not as denser as MWCNTs on the electrode surface. Figure 2c indicates the deposition of $\text{RuO}_x \cdot n\text{H}_2\text{O}$, which covers over MWCNTs, where patches of $\text{RuO}_x \cdot n\text{H}_2\text{O}$ formed on MWCNTs instead of beads which are shown in Figure 2b. This Figure 2c shows an obvious formation of MWCNTs- $\text{RuO}_x \cdot n\text{H}_2\text{O}$ hybrid film on ITO. Where, the $\text{RuO}_x \cdot n\text{H}_2\text{O}$ deposition over MWCNTs is more uniform

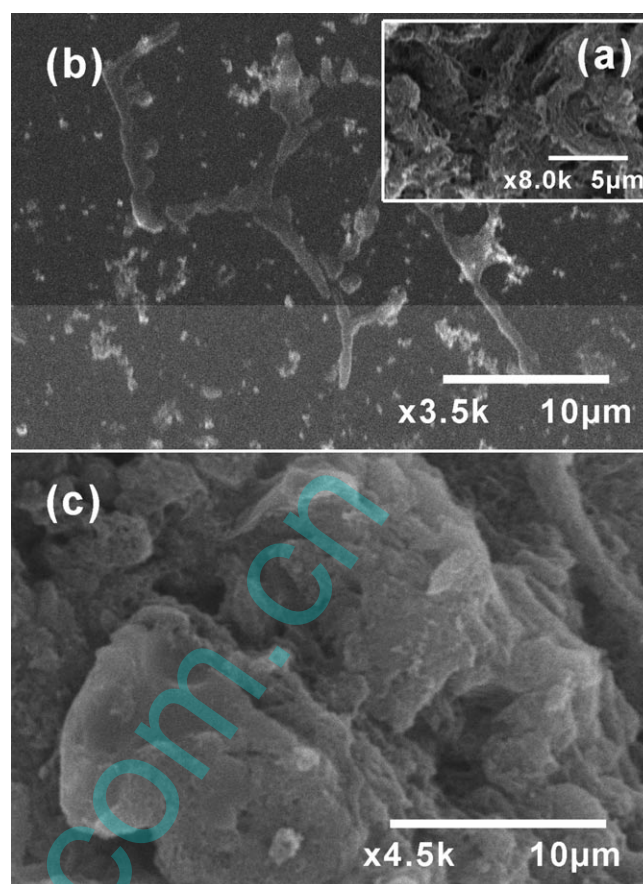


Fig. 2. SEM images of a) MWCNTs, b) $\text{RuO}_x \cdot n\text{H}_2\text{O}$ and c) MWCNTs- $\text{RuO}_x \cdot n\text{H}_2\text{O}$ hybrid films.

and high in concentration than the $\text{RuO}_x \cdot n\text{H}_2\text{O}$ on ITO. Similarly, Figure 3a and b shows the AFM images of only $\text{RuO}_x \cdot n\text{H}_2\text{O}$ and MWCNTs- $\text{RuO}_x \cdot n\text{H}_2\text{O}$ on ITO respectively. These AFM results are similar to SEM results for both $\text{RuO}_x \cdot n\text{H}_2\text{O}$ film and MWCNTs- $\text{RuO}_x \cdot n\text{H}_2\text{O}$ hybrid film.

3.3. Electroanalytical Studies of EP and NEP at $\text{RuO}_x \cdot n\text{H}_2\text{O}$, MWCNTs and MWCNTs- $\text{RuO}_x \cdot n\text{H}_2\text{O}$ Hybrid Film

Figure 4a and b are the electrocatalytic oxidation of EP and NEP respectively. The electrolytes used for the electrocatalytic reactions were pH 3 aqueous solutions. The CVs have been recorded at the constant time interval of 2 min with N_2 purging before the start of each experiment. The scan rate used for these electrocatalysis experiments is 10 mV s^{-1} . For comparison, in both sections of Figure 4, highest concentration of the analytes at bare GCE, $\text{RuO}_x \cdot n\text{H}_2\text{O}$ and MWCNTs are given along with the MWCNTs- $\text{RuO}_x \cdot n\text{H}_2\text{O}$ hybrid film in presence and absence of analytes. The CVs of MWCNTs- $\text{RuO}_x \cdot n\text{H}_2\text{O}$ hybrid film in Figure 4a and b exhibits reversible redox couples for $\text{RuO}_x \cdot n\text{H}_2\text{O}$ in the absence of analytes, upon the addition of analytes a new growth in the oxidation peak of EP and NEP

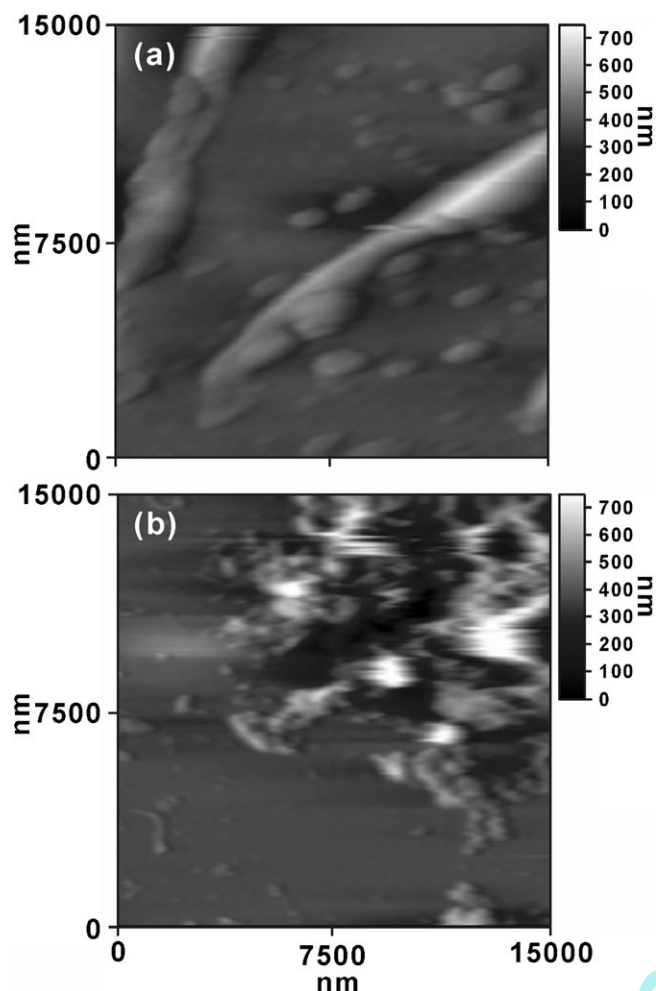
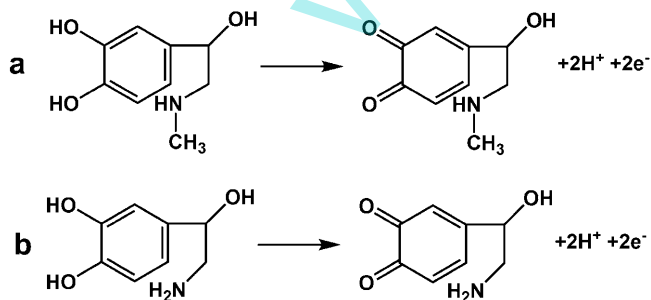


Fig. 3. AFM images of a) $\text{RuO}_x \cdot n\text{H}_2\text{O}$ and b) $\text{MWCNTs-RuO}_x \cdot n\text{H}_2\text{O}$ hybrid films.

appeared at $E_{\text{pa}} = 0.46$ V. These peak currents show that electrocatalytic oxidation of both the analytes took place at $\text{Ru}^{3+/4+}$, and could be represented by the Scheme 1.

During the electrocatalysis experiments, an increase in the concentration of analytes simultaneously produced a linear increase in the oxidation peak currents of the analytes with good film stability as shown in the insets in Figure 4a and b. It is obvious that, the $\text{MWCNTs-RuO}_x \cdot n\text{H}_2\text{O}$ hybrid film shows higher peak current for both the analytes when



Scheme 1. Electrochemical oxidation of a) EP and b) NEP.

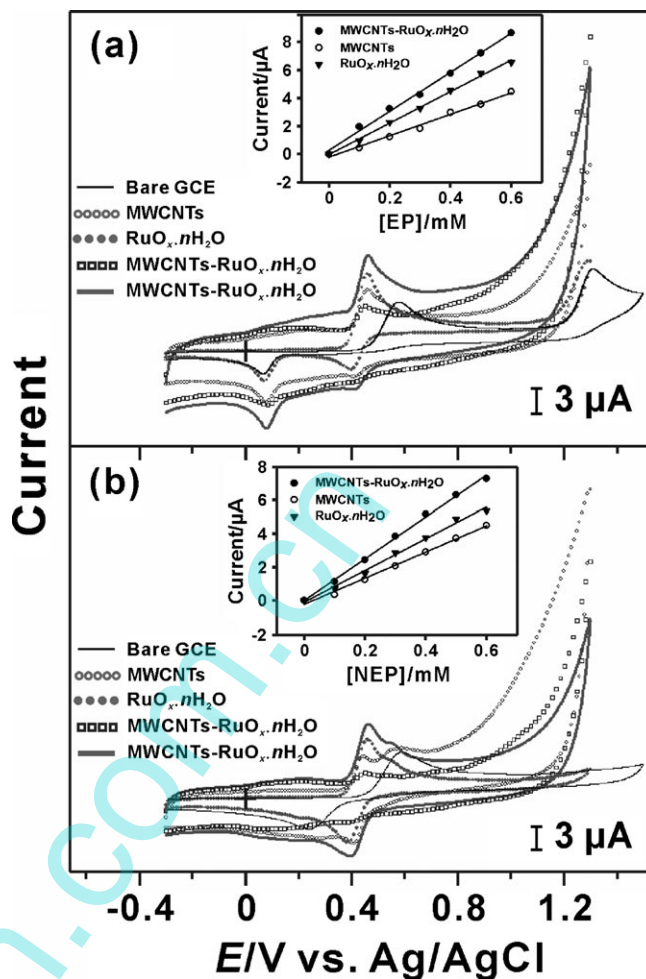


Fig. 4. CVs of a) EP and b) NEP at various electrodes using pH 3 aqueous solution at 10 mV s^{-1} . In both figures, $\text{MWCNTs-RuO}_x \cdot n\text{H}_2\text{O}$ hybrid film in the absence of analytes are shown with (square boxes line), where others are at the highest concentration of analytes. The inset in both figures is the plots of peak current vs. analyte concentration (0.1 to 0.6 mM) at different electrodes.

comparing to all other modified GCEs. The values of I_{pa} and E_{pa} for the analytes at different films are given in Table 2. The anodic peak currents are linear with the concentration of both analytes in the range of 0.1 to 0.6 mM, and the detection limit of $\text{MWCNTs-RuO}_x \cdot n\text{H}_2\text{O}$ hybrid film using CV technique is 0.1 mM for both the analytes. From the slopes of the linear calibration curves, the sensitivity of the various film modified GCEs and their correlation coefficient have been calculated and given in Table 3. These above results show that the sensitivity of $\text{MWCNTs-RuO}_x \cdot n\text{H}_2\text{O}$ hybrid film is higher for both the analytes. From the redox peaks of analytes given in Figure 4, k_s values has been calculated using Laviron theory, where the number of electrons involved are two [40, 41]. The k_s values for EP at bare GCE, $\text{RuO}_x \cdot n\text{H}_2\text{O}$, MWCNTs and $\text{MWCNTs-RuO}_x \cdot n\text{H}_2\text{O}$ are 1.8×10^{-5} , 1.9×10^{-4} , 2.1×10^{-4} and $2.4 \times 10^{-4} \text{ cm s}^{-1}$ respectively. Similarly, the k_s values for NEP at bare GCE, $\text{RuO}_x \cdot n\text{H}_2\text{O}$, MWCNTs and $\text{MWCNTs-RuO}_x \cdot n\text{H}_2\text{O}$ are 3.8×10^{-4} , 2.8×10^{-3} , 4.5×10^{-3} and $6.8 \times 10^{-3} \text{ cm s}^{-1}$

Table 2. Comparison of E_{pa} and I_{pa} of analytes obtained from electrocatalysis reactions using CV technique at different modified GCEs in pH 3 aqueous solution.

Analytes	Reaction type	E_p (V)				I_p (μ A)			
		[a]	[b]	[c]	[d]	[a]	[b]	[c]	[d]
EP	Oxidation	0.58	0.46	0.46	0.46	5.89	6.56	4.48	8.69
NEP	Oxidation	0.59	0.46	0.44	0.46	5.98	5.35	4.48	7.26

[a] bare GCE

[b] $\text{RuO}_x \cdot n\text{H}_2\text{O}$ modified GCE

[c] MWCNTs modified GCE

[d] MWCNTs- $\text{RuO}_x \cdot n\text{H}_2\text{O}$ modified GCE

respectively. Further, the interference studies have been carried out by varying the concentration of EP and NEP in presence of 1 mM of ascorbic acid at MWCNTs- $\text{RuO}_x \cdot n\text{H}_2\text{O}$ hybrid film (figures not shown) [39]. The results show that there is no change in the ascorbic acid peak current while increasing EP or NEP concentration, which reveals that there are no interference between the analytes and ascorbic acid. These results show that the MWCNTs- $\text{RuO}_x \cdot n\text{H}_2\text{O}$ hybrid film can be efficiently used for the detection of EP and NEP.

3.4. Flow Injection Analysis of EP and NEP at MWCNTs- $\text{RuO}_x \cdot n\text{H}_2\text{O}$ Hybrid Film

Figures 5a and b show the FIA studies of EP and NEP at MWCNTs- $\text{RuO}_x \cdot n\text{H}_2\text{O}$ hybrid film respectively, which have been synthesized on SPCE at similar conditions to that of GCE. Before the start of each experiment, the modified SPCE has been washed carefully with deionized water to remove the loosely bounded $\text{RuCl}_3 \cdot x\text{H}_2\text{O}$ on the modified SPCE. The carrier stream used was pH 3 aqueous solution with the flow rate of 0.03 mL s^{-1} and the volume of analytes injected at each cycle was $10 \mu\text{L}$. Figure 5a represents the successive addition of EP in the concentration range from 1 to $4 \mu\text{M}$ at the potential of 0.46 V. These optimized experimental conditions such as buffer and potential have been obtained from CV studies mentioned in section 3.1 and 3.3 respectively. Similarly, the optimization of flow rate for these FIA experiments has been done by conducting experiments in various flow rates and choosing the flow rate with has the highest response for both analytes. Similar to Figure 5a, Figure 5b represents the successive addition of NEP in the concentration range from 1 to $4 \mu\text{M}$ at the potential of 0.46 V. In both Figure 5a and b, the rapid amperometric response of the MWCNTs- $\text{RuO}_x \cdot n\text{H}_2\text{O}$

hybrid film is proportional to the respective analyte concentrations. The results obtained from both FIA have been plotted as shown in Figure 5 insets, where current vs. concentration of analytes are given. From the slopes of the linear calibration curves, sensitivity of the MWCNTs- $\text{RuO}_x \cdot n\text{H}_2\text{O}$ hybrid film have been calculated, and they are 688.3 and $888.6 \text{ nA } \mu\text{M}^{-1} \text{ cm}^{-2}$ for EP and NEP respectively. The performance of MWCNTs- $\text{RuO}_x \cdot n\text{H}_2\text{O}$

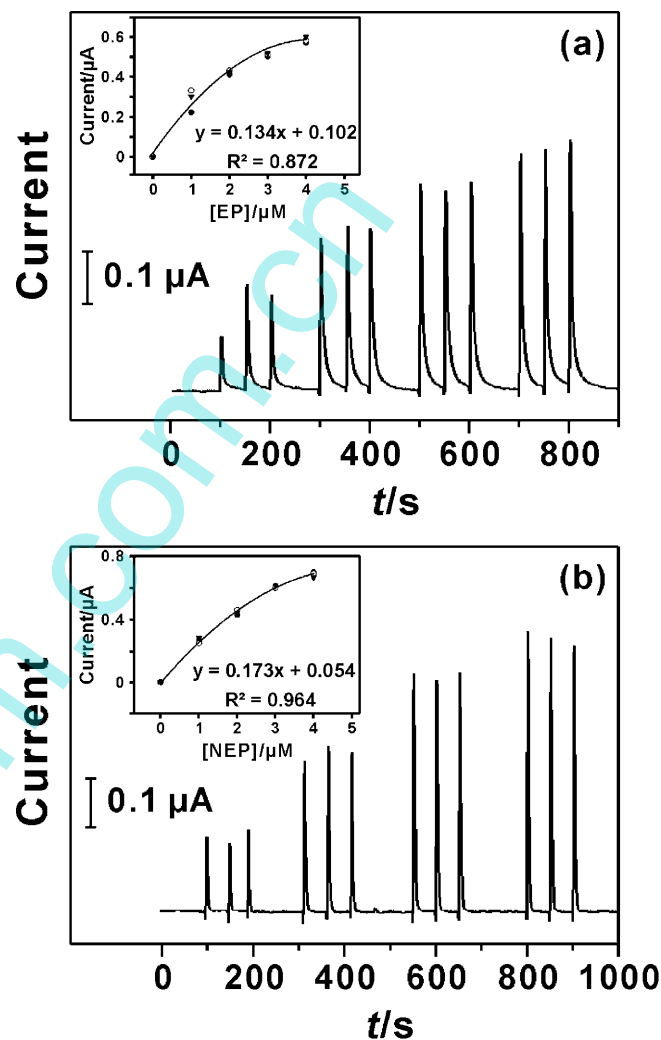


Fig. 5. FIA signal of MWCNTs- $\text{RuO}_x \cdot n\text{H}_2\text{O}$ hybrid film with various concentration of a) EP = 1, 2, 3 and $4 \mu\text{M}$; b) NEP = 1, 2, 3 and $4 \mu\text{M}$. The potential applied = 0.46 V for both EP and NEP, and the carrier stream used was pH 3 aqueous solution; flow rate = 0.03 mL s^{-1} and injected volume = $10 \mu\text{L}$. The insets show the plot of current vs. different concentration of analytes at MWCNTs- $\text{RuO}_x \cdot n\text{H}_2\text{O}$ hybrid film.

Table 3. Sensitivity and correlation co-efficient of different modified GCEs for analytes in CV technique. Values in brackets: slope's correlation coefficient

Analytes	Reaction type	Sensitivity ($\mu\text{A mM}^{-1} \text{ cm}^{-2}$)		
		$\text{RuO}_x \cdot n\text{H}_2\text{O}$	MWCNTs	MWCNTs- $\text{RuO}_x \cdot n\text{H}_2\text{O}$
EP	Oxidation	141.0 (0.9974)	95.9 (0.9904)	174.7 (0.9954)
NEP	Oxidation	118.1 (0.9932)	97.4 (0.9941)	155.6 (0.9976)

hybrid film modified SPCE has been tested using FIA by applying it to the determination of EP present in EP injection. The concentration added, found and the relative standard deviations are 0.2 μM , 0.19 μM and 1.28% respectively. The recovery of EP is $\approx 94.8\%$. These above results show that MWCNTs-RuO_x·nH₂O hybrid film is efficient for EP and NEP detection.

4. Conclusions

Novel hybrid material made of MWCNTs and RuO_x·nH₂O (MWCNTs-RuO_x·nH₂O) at GC, Au, ITO and SPC electrodes have been prepared, which are stable in aqueous solutions. The developed MWCNTs-RuO_x·nH₂O hybrid film for the electrocatalysis combines the advantages of ease of fabrication, high reproducibility and sufficient long-term stability. The EQCM results confirmed the incorporation of RuO_x·nH₂O on MWCNTs, and the SEM and AFM results show the difference between combinations of MWCNTs and RuO_x·nH₂O film's morphology. Further, MWCNTs-RuO_x·nH₂O hybrid film has excellent functional properties with good catalytic activity on EP and NEP. The experimental method of CV and FIA with hybrid film biosensor integrated into a GCE presented in this paper provides an opportunity for qualitative, quantitative characterization of EP and NEP. Therefore, this work establishes and illustrates, in principle and potential, a simple and novel approach for the development of EP and NEP voltammetric and amperometric sensor based on modified GCE.

5. Acknowledgement

This work was supported by The National Science Council and the Ministry of Education of Taiwan (Republic of China).

6. References

- [1] Z. Jusys, R. J. Behm, *Electrochim. Acta* **2004**, *49*, 3891.
- [2] L. Xiong, A. Manthiram, *Electrochim. Acta* **2004**, *49*, 4163.
- [3] E. V. Spinac'e, A. O. Neto, M. Linardi, *J. Power Sources* **2004**, *129*, 121.
- [4] Y. Takasu, T. Kawaguchi, W. Sugimoto, Y. Murakami, *Electrochim. Acta* **2003**, *48*, 3861.
- [5] K. W. Park, B. K. Kwon, J. H. Choi, I. S. Park, Y. M. Kim, Y. E. Sung, *J. Power Sources* **2002**, *109*, 439.
- [6] K. Shukla, R. K. Raman, N. A. Choudhury, K. R. Priolkar, P. R. Sarode, S. Emura, R. Kumashiro, *J. Electroanal. Chem.* **2004**, *563*, 181.
- [7] E. V. Spinac'e, A. O. Neto, T. R. R. Vasconcelos, M. Linardi, *J. Power Sources* **2004**, *137*, 17.
- [8] W. Zhou, Z. Zhou, S. Song, W. Li, G. Sun, P. Tsiakaras and Q. Xin, *Appl. Catal. B, Environ.* **2003**, *46*, 273.
- [9] L. Gao, H. Huang, C. Korzeniewski, *Electrochim. Acta* **2004**, *49*, 1281.
- [10] S. L. Gojkovic, T. R. Vidakovic, D. R. Durovic, *Electrochim. Acta* **2003**, *48*, 3607.
- [11] A. Yu, Z. Liang, J. Cho, F. Caruso, *Nano Lett.* **2003**, *3*, 1203.
- [12] Y. Xiao, H. X. Ju, H. Y. Chen, *Anal. Chim. Acta* **1999**, *391*, 73.
- [13] L. R. Hilliard, X. Zhao, W. Tan, *Anal. Chim. Acta* **2002**, *470*, 51.
- [14] M. Qhobosheane, S. Santra, P. Zhang, W. Tan, *Analyst* **2001**, *126*, 1274.
- [15] S. Dong, *Chemically Modified Electrodes*, Science Publishers, Beijing **1993**, p. 260.
- [16] R. Garjonyte, A. Malinauskas, *Sens. Actuators B* **1998**, *46*, 236.
- [17] S. M. Chen, C. M. Chan, *J. Electroanal. Chem.* **2003**, *543*, 161.
- [18] S. M. Chen, M. F. Lu, K. C. Lin, *J. Electroanal. Chem.* **2005**, *579*, 163.
- [19] N. R. de Tacconi, K. Rajeshwar, R. O. Lezna, *Electrochim. Acta* **2000**, *45*, 3403.
- [20] K. M. Jeerage, W. A. Steen, D. T. Schwartz, *Chem. Mater.* **2002**, *14*, 530.
- [21] M. Jeyalakshmi, F. Scholz, *J. Power Sources* **2000**, *91*, 217.
- [22] J. Wang, M. Musameh, *Anal. Chim. Acta* **2004**, *511*, 33.
- [23] H. Cai, X. Cao, Y. Jiang, P. He, Y. Fang, *Anal. Bioanal. Chem.* **2003**, *375*, 287.
- [24] A. Erdem, P. Papakonstantinou, H. Murphy, *Anal. Chem.* **2006**, *78*, 6656.
- [25] Q. Li, J. Zhang, H. Yan, M. He, Z. Liu, *Carbon* **2004**, *42*, 287.
- [26] J. Zhang, J. K. Lee, Y. Wu, R. W. Murray, *Nano Lett.* **2003**, *3*, 403.
- [27] M. Zhang, K. Gong, H. Zhang, L. Mao, *Biosens. Bioelectron.* **2005**, *20*, 1270.
- [28] R. J. Chen, Y. Zhang, D. Wang, H. Dai, *J. Am. Chem. Soc.* **2001**, *123*, 3838.
- [29] J. Wang, T. Tangkuaram, S. Loyprasert, T. Vazquez-Alvarez, W. Veerasai, P. Kanatharana, P. Thavarungkul, *Anal. Chim. Acta* **2007**, *581*, 1.
- [30] J. Wang, J. Dai, T. Yarlagadda, *Langmuir* **2005**, *21*, 9.
- [31] U. Yogeswaran, S. M. Chen, *Sensors* **2008**, *8*, 290.
- [32] M. H. Sorouraddin, J. L. Manzoori, E. Kargarzadeh, A. M. H. Shabani, *J. Pharm. Biomed. Anal.* **1998**, *18*, 877.
- [33] M. E. El-Kommos, F. A. Mohamed, A. S. K. Khedr, *J. Assoc. Off. Anal. Chem.* **1990**, *73*, 516.
- [34] Y. Yan, M. Zhang, K. Gong, L. Su, Z. Guo, L. Mao, *Chem. Mater.* **2005**, *17*, 3457.
- [35] U. Yogeswaran, S. M. Chen, *Sens. Actuators, B: Chem.* **2008**, *130*, 739.
- [36] P. Shakthivel, S. M. Chen, *Biosens. Bioelectron.* **2007**, *22*, 1680.
- [37] U. Yogeswaran, S. M. Chen, S. H. Li, *Electroanalysis* **2008**, *20*, 2324.
- [38] U. Yogeswaran, S. M. Chen, *Electrochim. Acta* **2007**, *52*, 5985.
- [39] U. Yogeswaran, S. M. Chen, *Sens. Actuator B* **2008**, *130*, 739.
- [40] E. Laviron, *J. Electroanal. Chem.* **1979**, *101*, 19.
- [41] A. Guiseppi-Elie, S. Brahim, G. Wnek, R. Baughman, *NanoBiotechnology* **2005**, *1*, 83.